Article

Discovery Medicine 2024; 36(184): 1041–1053
https://doi.org/10.24976/Discov.Med.202436184.97

GSK-126 Enhances All-Trans-Retinoic Acid (ATRA) Response in Hepatocellular Carcinoma (HCC) by Upregulating *RARG* Expression

Zhidan Liu[1,2], Yongxia Zheng[2,*]

[1]School of Basic Medicine, Zhejiang Chinese Medical University, 310000 Hangzhou, Zhejiang, China
[2]Medical Molecular Biology Laboratory School of Medicine, Jiaxing University, 314001 Jiaxing, Zhejiang, China
*Correspondence: zhengyongxiajx@outlook.com (Yongxia Zheng)
Published: 20 May 2024

Background: Hepatocellular carcinoma (HCC) stands out as one of the most prevalent malignant tumors globally. The combination of all-trans-retinoic acid (ATRA) with FOLFOX chemotherapy has shown promise in enhancing the prognosis of HCC patients. ATRA, serving as a chemosensitizing agent, presents novel possibilities for therapeutic applications. Nevertheless, the responsiveness of HCC cells to ATRA varies. The epigenetic modifier—GSK-126 is currently under investigation as a potential antitumor drug. Our aim is to explore the molecular mechanisms underlying the diverse sensitivity of HCC patients to ATRA, and to propose a new combination regimen. This research aims to lay the groundwork for personalized medication approaches for individuals with HCC.

Methods: A cell model with low expression of retinoic acid receptor Alfa (*RARA*), retinoic acid receptor belta (*RARB*), and retinoic acid receptor gamma (*RARG*) was established through siRNA interference. The impact of reduced expression of *RARA*, *RARB*, and *RARG* on the half maximal inhibitory concentration (IC_{50}) of ATRA in Hep3B cells was assessed using the 3-(4,5-Dimethyl-2-Thiazolyl)-2,5-Diphenyl Tetrazolium Bromide (MTT) cytotoxicity assay. Flow cytometry revealed that *RARG* emerged as the key receptor influencing the combination's sensitivity. Conducting ChIP-qPCR analysis on genomic DNA from HCC cells through relevant websites demonstrated enrichment of the trimethylation modification of lysine 27 on histone H3 (H3K27me3) upstream of the *RARG* promoter. ChIP-PCR assay confirmed that GSK-126 could diminish H3K27me3 levels on the *RARG* promoter, subsequently elevating *RARG* expression. The synergistic efficacy of GSK-126 and ATRA was validated through MTT assay, flow cytometry apoptosis assay, cell cycle assay, and cell scratch assay.

Results: Our study unveiled that the insensitivity of HCC cells to ATRA could be linked to the low expression of *RARG*. ChIP-qPCR analysis illuminated that GSK-126 activated *RARG* expression by diminishing H3K27me3 enrichment in the *RARG* promoter region. Consequently, the concurrent administration of ATRA and GSK-126 to hepatoma cells exhibited a synergistic effect, inhibiting cell proliferation, inducing cell apoptosis, and reducing the proportion of cells in the S-phase.

Conclusion: Our findings emphasize that the synergistic action of GSK-126 and ATRA enhances the sensitivity of HCC cells by upregulating the expression of *RARG*. This presents a potential foundation for personalized HCC treatment.

Keywords: hepatocellular carcinoma; synergistic medication; GSK-126; ATRA; RARG

Introduction

Hepatocellular carcinoma (HCC) stands as a prevalent malignant tumor worldwide, with medication remaining a crucial treatment avenue for advanced HCC patients ineligible for surgery [1]. The inherent heterogeneity of HCC results in varying sensitivity to medication regimens among patients [2,3]. It is imperative to comprehend the factors influencing sensitivity to medication for the purpose of selecting personalized treatment regimens.

Previous research has demonstrated the effectiveness of combining all-trans-retinoic acid (ATRA) with cisplatin [4] or oxaliplatin, fluorouracil, and leucovorin (FOLFOX4) [5] in improving prognoses for the majority of HCC cases, prompting speculation about ATRA's potential as a chemosensitive medication and opening new avenues for therapeutic applications. However, the susceptibility of HCC cells to ATRA varies. ATRA, a derivative of vitamin A, exhibits anticancer efficacy in various malignancies, including HCC [6].

Notably, ATRA binds to the nuclear receptor retinoic acid receptor (RAR), enhancing its transcription factor activity and activating downstream target genes [7]. RAR comprises three subtypes: RARα, RARβ, and RARγ [7,8]. The specific roles or potential competition among RARα, RARβ, and RARγ in mediating the effects of ATRA remain unclear. Existing studies have indicated that the ATRA pathway is compromised by decreased expression of ATRA receptors [9,10]. Therefore, it becomes crucial to identify the primary receptors responsible for mediating ATRA's

inhibitory effects on hepatoma cell proliferation. In this study, the retinoic acid receptor gamma (*RARG*) gene, encoding RXRγ, emerges as a key player in determining liver cancer sensitivity to ATRA.

ChIP-seq analysis conducted by Gerstein M has illuminated that the expression of *RARG* is influenced by the trimethylation modification of lysine 27 on histone H3 (H3K27me3), a marker associated with transcriptional repression [11]. This modification is catalyzed by enhancer of zeste 2 polycomb repressive complex 2 subunit (EZH2), the key catalytic subunit of the polycomb repressive complex 2 (PRC2) [12]. Notably, EZH2 overexpression is frequently observed in advanced and metastatic cancers [13], rendering it an attractive target in HCC patients. Various EZH2 inhibitors have been investigated in clinical studies, aiming to reduce global levels of H3K27me3 [14].

GSK-126, a highly selective small molecule inhibitor of EZH2, has shown promise as an anticancer drug in the treatment of non-Hodgkin lymphoma [15], solid tumors [16,17], and multiple myeloma [18]. Currently, it is in the experimental stage of clinical development [19]. In this study, we delve into the synergistic anti-tumor effects and the underlying mechanism based on the combination of GSK-126 and ATRA in human HCC cell lines.

Materials and Methods

ATRA and GSK-126

All-trans-retinoic acid powder (>98% purity, 2207091, Zeye Biotechnology, Shanghai, China) and GSK-126 powder (>98% purity, C22M11L113783, Yuanye Biotechnology, Shanghai, China) were dissolved in DMSO (ST038, Beyotime, Nanjing, China). The ATRA stock solution concentration was 100 mM, while the GSK-126 stock solution concentration was 10 mM.

Cell Culture and siRNA Transfection

We obtained hepatoma cell lines Hep3B (TCHu106), HepG2 (SCSP-510), and SMMC-7721 (TCHu 72) from the Institute of Cellology affiliated with the Chinese Academy of Sciences in Shanghai. The SMMC-7721 cell line was cultured in RPMI-1640 medium, supplemented with 10% fetal bovine serum and a 1% penicillin-streptomycin mix, both sourced from Shenghang Biologics in Nanjing. On the other hand, both Hep3B and HepG2 were cultured in high-glucose DMEM medium, supplemented similarly but obtained from Biologics, Nanjing. All cell lines were consistently maintained in an incubator set at 37 °C, with a humidity level nearing saturation and an atmosphere containing 5% CO_2. The identification of Hep3B, HepG2 and SMMC-7721 cell lines was confirmed by cell line authenticationby Short Tandem Repeat (STR) profiling and mycoplasma testing was conducted for all cell lines.

For the transfection procedures, we utilized the Lipofectamine™ RNAiMAX transfection agent (product code: 13778150) from Invitrogen, Carlsbad, CA, USA. A siRNA obtained from Sangon, Shanghai with a concentration of 50 nM was employed, following the outlined protocol. The siRNA sequences, designed by Shanghai Genechem Pharmaceutical Technology, are provided in Table 1.

Table 1. siRNA sequences.

Gene	Sequence (5′-3′)
hRARA-1 sense	CACCAGCUUCCAGUUAGUGGAUAUA
hRARA-1 antisense	UAUAUCCACUAACUGGAAGCUGGUG
hRARA-2 sense	CAGCUUCCAGUUAGUGGAUAUAGCA
hRARA-2 antisense	UGCUAUAUCCACUAACUGGAAGCUG
hRARB-1 sense	GACAAAUCAUCAGGGUACCACUAUG
hRARB-1 antisense	CAUAGUGGUACCCUGAUGAUUUGUC
hRARB-2 sense	CACCGAGAUAAGAACUGUGUUAUUA
hRARB-2 antisense	UAAUAACACAGUUCUUAUCUCGGUG
hRARG-1 sense	GACAAGUCCUCUGGCUACCACUAUG
hRARG-1 antisense	CAUAGUGGUAGCCAGAGGACUUGUC
hRARG-2 sense	CAUGUCCAAGGAAGCUGUGCGAAAU
hRARG-2 antisense	AUUUCGCACAGCUUCCUUGGACAUG
NC sense	UUCUCCGAACGUGUCACGUTT
NC antisense	ACGUGACACGUUCGGAGAATT

RARA, retinoic acid receptor Alfa; *RARB*, retinoic acid receptor belta; *RARG*, retinoic acid receptor gamma.

Quantitative Real-Time Polymerase Chain Reaction (qRT-PCR) Experiments

Cellular RNA was isolated using the TRIzol reagent sourced from Edland, Beijing. Subsequently, mRNA extraction underwent cDNA conversion through the Perfect Real Time Toolkit by Takara, Japan. This conversion process was initiated at 37 °C for 15 minutes, followed by transcriptase inactivation at 85 °C briefly for 5 seconds, and concluded with preservation at 4 °C. Quantitative assessment via quantitative real-time polymerase chain reaction (qRT-PCR) utilized the SYBR Premix Ex Taq II, also a Takara product. The PCR cycling commenced with an initial 30-second phase at 95 °C, followed by 40 iterations alternating between 5-second durations at 95 °C and half-minute phases at 60 °C. The relative expression of mRNA was calculated using the $2^{-\Delta\Delta Ct}$ method, with β-actin expression as the internal control. Primer sets for this research were procured from Shanghai Sangon Biotechnology, with their sequences explicitly detailed in Table 2.

Western Blotting Assay

Three hepatoma cell lines, Hep3B, HepG2, and SMMC-7721, were seeded in 6-well plates, and the experiment was divided into five groups. The Control group received no treatment, the DMSO group was treated with a final concentration of 5 µM DMSO, the ATRA group was treated with a final concentration of 25 µM ATRA, the GSK-126 group was treated with a final concentration of 5 µM GSK-126, and the Combination group was co-treated

Table 2. Primer sequences.

Gene	Sequence (5′-3′)
hRARG Forward	GCAGAGTCAGTGTGCGGTTT
hRARG Reverse	AGTCGCTCCTTATTGGTGGC
hRARB Forward	TCTGAGTGAAAAGATTGTGGCA
hRARB Reverse	TGGCATCGATTCCTGGTGAC
hRARA Forward	CCAGCCACTGTGAGAAACGA
hRARA Reverse	CTTGGCGAACTCCACAGTCT
β-actin Forward	TTGTGATGGACTCCGGAGAC
β-actin Reverse	TGATGTCACGCACGATTTCC
(ChIP) RARG Forward	GCGATACAGCGGGGTAGAG
(ChIP) RARG Reverse	ATCCACTACTGTGTTGGCTCC

with 25 μM ATRA and 5 μM GSK-126. After 48 hours of treatment, total proteins were extracted using 60 μL of RIPA. The total protein concentration was quantified using the BCA Protein Assay Kit (P0012, Beyotime, Nanjing, China).

Post boiling, 20 μg of these proteins were subjected to SDS-PAGE and then transferred to a PVDF membrane. The membrane was blocked using 5% skim milk for two hours and rinsed thrice using 1×TBST, with each rinse lasting 5 minutes. The membrane was incubated overnight at 4 °C with the primary antibodies. Following this incubation, the primary antibody was removed, and the membrane was exposed to either horseradish-peroxidase-tagged goat anti-rabbit (A0277, 1:2000, Beyotime, Nanjing, China) or horseradish-peroxidase-tagged goat anti-mouse (A0286, 1:2000, Beyotime, Nanjing, China) secondary antibodies for two hours. Visualization was achieved through ECL (A38554, Thermo Fisher Scientific, MA, USA) after a final wash. β-actin served as the normalization control.

The antibodies used in this study included β-Actin (AF5003, 1:1000) from Beyotime (Nanjing, China), RARG (sc-7387, 1:1000) from Santa Cruz Biotechnology (Santa Cruz, CA, USA), and H3K27me3 (mAbcam 6002, 1:1000) from Abcam (Cambridge, MA, USA). The signals were detected using Amersham Imager 680 (29270771, GE Health, MA, USA). ImageJ software (ImageJ 1.53K, Wayne Rasband and contributors National Institutes of Health, Bethesda, MD, USA) was employed to quantify the band density of each protein and the corresponding β-actin. The relative expression of each protein was analyzed by the gray scale ratio (target protein/β-actin).

ChIP Assay

Following the guidelines provided by the ChIP Assay Kit (P2078, Beyotime, Nanjing, China), a ChIP assay was conducted. The experimental design included three distinct groups: a control cohort receiving no interventions, a DMSO cohort exposed to a 5-μM terminal DMSO concentration, and a GSK-126 cohort exposed to a terminal concentration of 0.1 μM GSK-126. For each category, 1×10^7 cells were cultured in dishes with a 10 cm diameter, and after 72-hour drug exposure, they were fixed using 1% formaldehyde. These cells were then collected using a solution comprising 100 mmol/L Tris-Cl (pH 9.4) and 10 mmol/L DTT, followed by three washes in chilled PBS.

Post-wash, cell lysis was induced by adding lysate fortified with 1 mM PMSF. Subsequent ultrasonication was performed in intervals for 10 seconds with 30% energy output, repeated ten times. This led to the generation of chromatin fragments ranging between 300–1000 bp. Chromatin segments were then isolated from the resulting solution and coupled with either H3K27me3-specific mouse monoclonal antibody or IgG, serving as a negative control. For quantification, DNA fragments bound to H3K27me3 were amplified using *RARG* promoter-specific primers by using qPCR method. Detailed primer sequences are available in Table 2.

3-(4,5-Dimethyl-2-Thiazolyl)-2,5-Diphenyl Tetrazolium Bromide (MTT) Assay

Hep3B, HepG2, and SMMC-7721, all hepatocellular carcinoma cell strains, were seeded in 96-well plates with an initial count of 1×10^4 cells per well. The experiment comprised four groups: DMSO group treated with a final concentration of 5 μM DMSO, ATRA group treated with gradient concentrations of 20 μM, 40 μM, 80 μM, 160 μM, 320 μM ATRA, GSK-126 group treated with gradient concentrations of 4 μM, 8 μM, 16 μM, 32 μM, 64 μM GSK-126, and combination group co-treated with a mixture of ATRA and GSK-126 at a 5:1 ratio according to the above-mentioned concentration gradient for each.

After a 24-hour drug exposure, we added the 3-(4,5-Dimethyl-2-Thiazolyl)-2,5-Diphenyl Tetrazolium Bromide (MTT) solution (ST316, Beyotime, Nanjing) for an hour at 37 °C. Post-incubation, the supernatant was removed, and 100 μL of DMSO was added to induce formazan dissolution. A microplate reader then measured the optical density at 490 nm. The blank group was used to detect the optical density (OD) value of the solution, and the blank group was set to exclude the effect of the reagent on the OD value.

Cell viability (%) was calculated using the formula: (drug group OD value – blank group OD value)/(DMSO group OD value – blank group OD value) multiplied by 100%.

Scratch Experiments

In our study, hepatoma cell strains including Hep3B, HepG2, and SMMC-7721 were plated in 24-well plates with an initial density of 1×10^5 cells per well. The experiment comprised five groups: Control group subjected to no treatment, DMSO group treated with a final concentration of 5 μM DMSO, ATRA group treated with a final concentration of 25 μM ATRA, GSK-126 group treated with a final concentration of 5 μM GSK-126, and combination group co-treated with 25 μM ATRA and 5 μM GSK-126.

When cells covered approximately 90% of the plate's surface area, a 200-μL sterile pipette tip was used to create a

scratch. Subsequently, the cells underwent drug treatments. Observations were made using an inverted microscope at the onset of drug treatment and 24 hours thereafter, capturing the cellular responses photographically. The variance in the scratch's width was quantitatively assessed using Image J. To further evaluate the cell movement rate, we utilized Graphpad Prism 7.0 (GraphPad software, La Jolla, CA, USA), employing the formula: Cell Mobility = [(Initial scratch width at 0 h – Width post 24 h)/Initial scratch width at 0 h] multiplied by 100%.

Flow Cytometry Analysis of Apoptosis and Cell Cycle

In this investigation, hepatoma cell strains Hep3B, HepG2, and SMMC-7721 were inoculated in 6-well plates at an initial density of 5×10^5 cells per well. The study design included five distinct sets: an untreated Control set, a DMSO set exposed to a concluding 5-µM DMSO concentration, an ATRA group exposed to 25-µM of ATRA, a GSK-126 set that encountered a 5-µM GSK-126 concentration, and a combination group receiving both 25-µM ATRA and 5-µM GSK-126 treatments.

A day post the drug exposure, cells were harvested and subjected to staining protocols outlined in the annexin V-FITC apoptosis assay kit (C1062M, Beyotime Biotechnology, Nanjing) and the cell cycle assay kit (C1052, Beyotime Biotechnology, Nanjing). Flow cytometry, facilitated by FlowJo 7.6 software (Becton, Dickinson and Company, Sussex County, NJ, USA) enabled the detection of both apoptosis rates and cell cycle progression. The rate of apoptosis was determined with the formula: apoptosis rate% = (count of initial apoptotic cells + count of advanced apoptotic cells)/the total cell count $\times$ 100%. Additionally, we scrutinized the distribution of hepatoma cell strains across different cell cycle phases, namely G1, S, and G2/M.

Genes Associated with HCC

From several databases, including OncoDB. HCC (http://oncodb.hcc.ibms.sinica.edu.tw), Genecard (https://www.genecards.org/), Therapeutic Target (https://db.idrblab.net/ttd/), DisGeNET (https://www.disgenet.org/), OMIN, PharmGKB (https://www.pharmgkb.org/), and CTD (https://ctdbase.org/), we identified a total of 922 genes associated with HCC (**Supplementary Table 1**). The OncoDB.HCC database was specifically employed because it contained both microarray data and corresponding literature for experimental validation. For the Genecard database, genes with a correlation coefficient (Score >16.5) were filtered. Using "HCC" and "HOMO" as search terms in the Therapeutic Target and OMIN databases, we identified genes solely targeting liver cancer. In the PharmGKB database, a search resulted in 6550 potential liver cancer target genes; of these, we focused on the top 10% as our primary liver cancer gene targets. Lastly, in the CTD database, only genes with an Inference Score exceeding 100 were considered, following a search using "liver cancer" and "HOMO". After consolidating the findings from these databases, we eliminated any overlapping or duplicate genes.

GSK-126 Target Gene and ATRA Target Gene

There are 400 target genes of GSK-126 (**Supplementary Table 2**) and 540 target genes of ATRA (**Supplementary Table 3**) screened from four databases: SwissTargetPrediction database (http://www.swisstargetprediction.ch/), CTD database (https://ctdbase.org/), Pharmmapper database (https://www.lilab-ecust.cn/pharmmapper/) and Genecard database (https://www.genecards.org/).

The filtering criteria for the SwissTargetPrediction database is probability >0. GeneCards database screening criteria for GSK-126 target is Relevance score >0, and for ATRA target is Relevance score >1.7. All genes obtained from CTD database for GSK-126 using GSK-126, HOMO as keywords are considered target genes, and for ATRA targets, the keywords used are ATRA, HOMO, with Interaction Count >10 as the filtering condition. In the Pharmmapper database, GSK-126 and ATRA two-dimensional structure diagrams and three-dimensional structure diagrams are used as screening key volumes respectively, with Norm Fit >0 as the screening standard.

Screening of Hepatoma-GSK-126-ATRA Cross Target Genes and Protein-Protein Interaction (PPI) Analysis

We utilized the online platform jvenn [20], accessible at https://jvenn.toulouse.inrae.fr/app/index.html, for the HCC-GSK-126-ATRA target gene identification. This analysis pinpointed 81 genes as shared targets for both HCC and the compounds GSK-126 and ATRA. Furthermore, to delve into protein-protein interactions, we harnessed the STRING database [21], available at https://string-db.org/ (version 11.5). Notably, the interactions exhibited a robust correlation coefficient of 0.8, with the analysis set to the Homo sapiens species.

Statistical Analysis

For statistical evaluations and graphical representations, we employed GraphPad Prism 8.0 software (GraphPad software, La Jolla, CA, USA), which also facilitated the computation of the half maximal inhibitory concentration (IC_{50}) values. Dose-response curves and the derivation of combination indices (CI) were achieved using CompuSyn software (Version 3.0.1) (ComboSyn, Inc., Paramus, NJ, USA). Each of these experimental procedures was executed on three separate occasions. The outcomes of these experiments are presented as the mean value complemented by the standard deviation ($\bar{x} \pm$ SD). To assess significant disparities among the mean scores of various groupings, one-way Analysis of Variance (ANOVA) was conducted and followed by Tukey's post hoc test. Any resulting p-value less than 0.05 was considered significant.

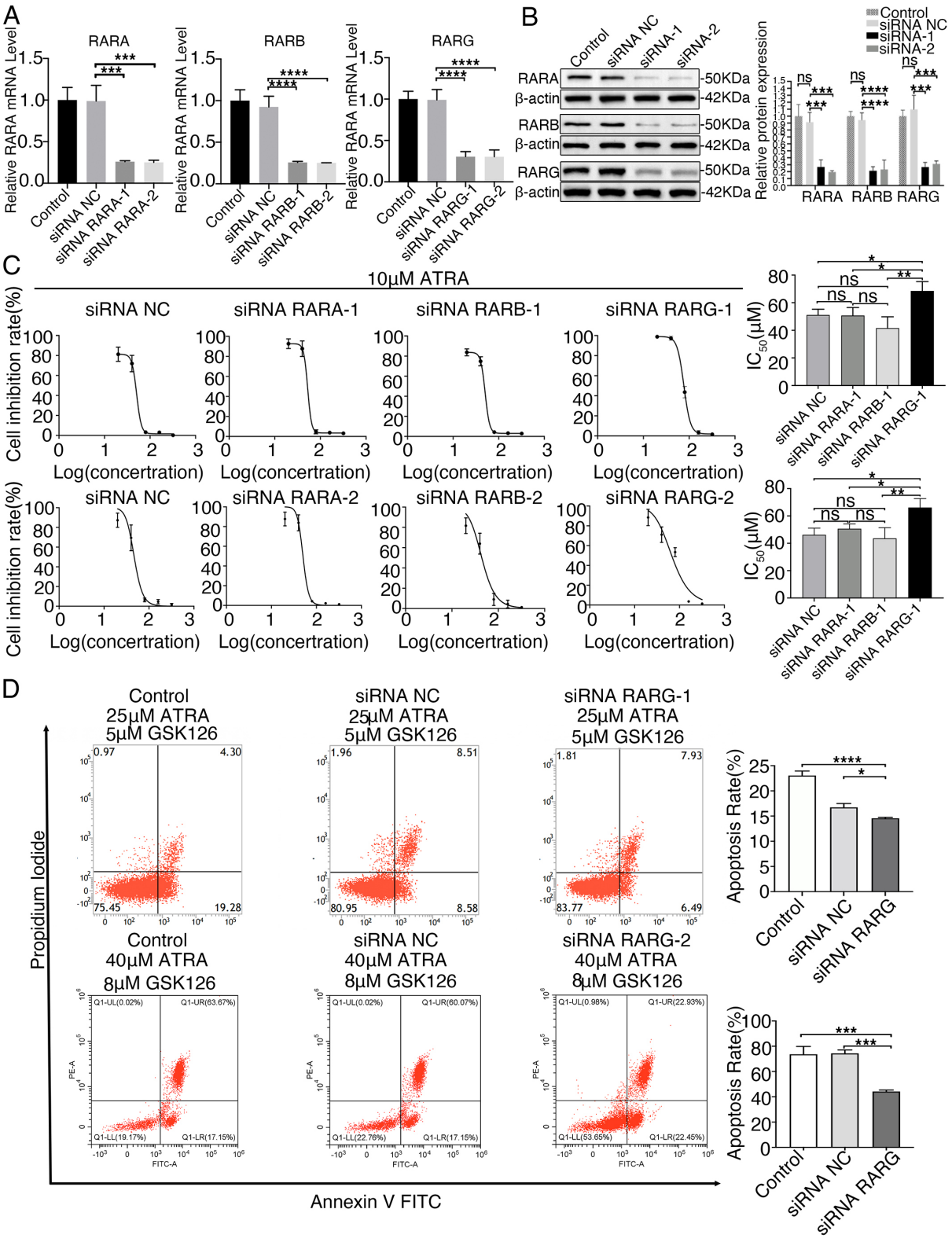

Fig. 1. RARG plays an important role in the inhibitory effect of all-trans-retinoic acid (ATRA) and GSK126 on hepatocellular carcinoma (HCC). (A) siRNA (*RARA*, *RARB*, *RARG*) interference efficiency in Hep3B cells by quantitative real-time polymerase chain reaction (qRT-PCR). (B) siRNA (*RARA*, *RARB*, *RARG*) interference efficiency in Hep3B cells by western blotting. (C) The curve graphs represent ATRA half maximal inhibitory concentration (IC_{50}) after siRNA NC, siRNA *RARA*, siRNA *RARB* and siRNA *RARG* interference in Hep3B cells, respectively, and the histograms show ATRA IC_{50} of siRNA interference in Hep3B cell lines. (D) Flow cytometry apoptosis assay was employed to detect the effect of *RARG* on the killing effect of GSK126 combined with ATRA. N = 3. ns: not statistically; *$p < 0.05$; **$p < 0.01$; ***$p < 0.001$; ****$p < 0.0001$.

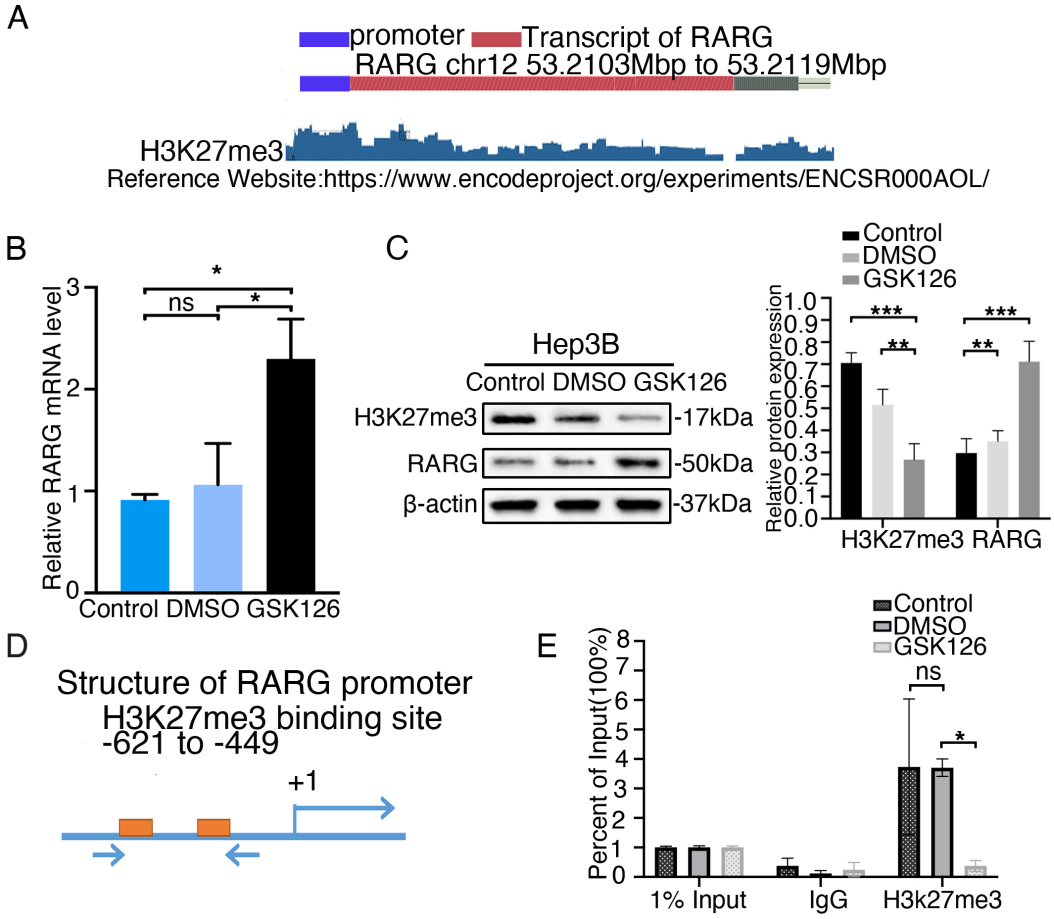

Fig. 2. RARG expression is regulated by GSK-126 in Hep3B cells. (A) The trimethylation modification of lysine 27 on histone H3 (H3K27me3) enrichment analysis of *RARG* chromatin and *RARG* chromatin was enriched for H3k27me3. (B) Quantitative real-time polymerase chain reaction (qRT-PCR) was used to detect the expression of *RARG* in Hep3B cells treated with 0.1 μM GSK-126, and GSK-126 promoted the significant expression of *RARG*. (C) Expression of H3k27me3 and RARG in Hep3B cells treated with GSK-126 was detected by western blotting, GSK126 inhibited the protein expression of H3K27me3 and increased the protein expression of RARG. (D) Primer design sites for ChIP experiment. (E) ChIP experiments confirmed that H3k27me3 was suppressed, and *RARG* promoter expression was decreased. N = 3. ns: not statistically; *$p < 0.05$; **$p < 0.01$; ***$p < 0.001$.

Results

RARG is the Main Receptor Mediating Cancer Inhibitory Effect of ATRA and GSK126

To determine the primary receptor among *RARA*, *RARB*, and *RARG* for ATRA, we conducted RNA interference experiments in Hep3B cell lines. We individually downregulated the expression of *RARA*, *RARB*, and *RARG* with siRNA and examined the mRNA level and protein expression of RARA, RARB, and RARG after interference (Fig. 1A,B). Subsequently, we treated the cells with DMSO and ATRA. We assessed the impact of interfering with different RAR receptors on the half-maximal inhibitory concentration (IC_{50}) of ATRA using the MTT assay. The IC_{50} results (Fig. 1C) showed that the IC_{50} of ATRA on hepatoma cells in the siRNA *RARG* group was significantly higher than that in the siRNA *RARA* ($p < 0.05$) and *RARB* ($p < 0.05$) groups. These results suggested that compared with *RARA* and *RARB*, *RARG* is the main receptor mediating the inhibitory effect of ATRA on hepatoma cells.

Furthermore, flow cytometry (Fig. 1D) showed that compared with the control ($p < 0.05$) and siRNA NC ($p < 0.05$) groups, the siRNA *RARG* group significantly reduced the killing effect of ATRA and GSK126 combined treatment. Collectively, these results suggested that *RARG* is the main receptor mediating the cancer inhibitory effect of ATRA and GSK126.

GSK-126 Promotes Expression of RARG

ChIP-seq analysis (http://www.encodeproject.org/) demonstrated the enrichment of H3K27me3 upstream of the *RARG* gene promoter (Fig. 2A). Based on this finding, we hypothesized that GSK-126, an EZH2 inhibitor, could reduce the level of H3K27me3 in the *RARG* promoter region, thereby promoting the transcription of the *RARG* gene.

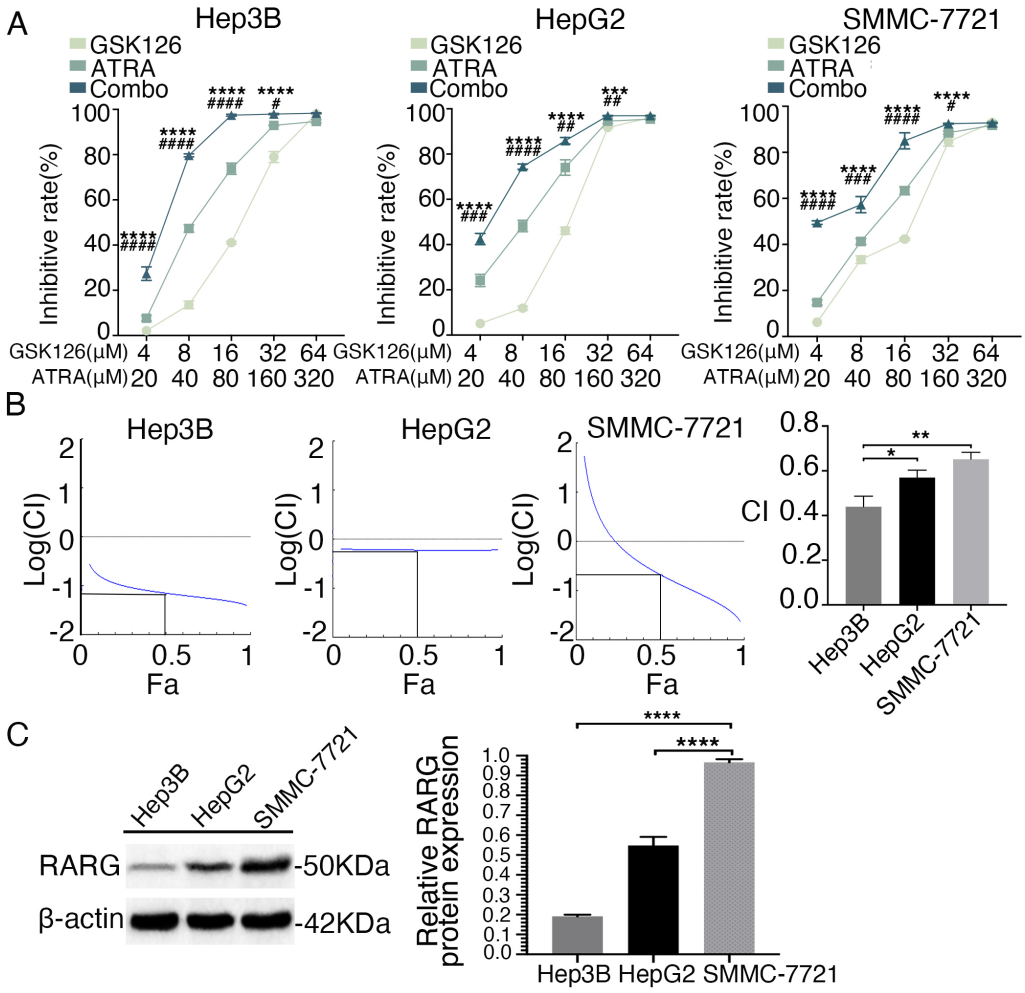

Fig. 3. GSK-126 combined with all-trans-retinoic acid (ATRA) synergistically inhibits the proliferation of Hep3B, HepG2 and SMCC-7721 cells. (A) 3-(4,5-Dimethyl-2-Thiazolyl)-2,5-Diphenyl Tetrazolium Bromide (MTT) assay confirmed a synergistic inhibitory effect of GSK-126 combined with ATRA on proliferation in HepG2, SMMC-772 and Hep3B. (B) CI values of combination drugs in Hep3, HeG2, SMMC-7721. (C) Western blotting was used to detect the protein expression of RARG in Hep3B, HepG2 and SMMC-772. N = 3. *$p < 0.05$; **$p < 0.01$; ***$p < 0.001$; ****$p < 0.0001$. vs. combo GSK-126. #$p < 0.05$; ##$p < 0.01$; ###$p < 0.001$; ####$p < 0.0001$. vs. combo ATRA.

To investigate the impact of EZH2 inhibitors on *RARG* regulation, the HCC cell line Hep3B was treated with GSK-126, an EZH2 inhibitor. RT-PCR and western blotting analysis demonstrated that GSK-126 increased the expression of RARG at both the mRNA and protein levels (Fig. 2B,C). Moreover, the expression of H3K27me3 protein was reduced in the GSK126 group compared with the control group ($p = 0.0017$) and DMSO group ($p = 0.0112$) (Fig. 2C). Collectively, these findings indicated that GSK-126 enhances the mRNA and protein level of RARG by reducing the H3K27me3 level in the Hep3B cell line.

Additionally, to determine whether GSK-126 enhances *RARG* expression by reducing the level of H3K27me3 enrichment in the upstream promoter region of *RARG*, ChIP-PCR analysis was performed to analyze H3K27me3 modification in the *RARG* promoter region (Fig. 2D). The results revealed a significant decrease in the PCR product in the GSK-126 group compared to the DMSO group. The results confirmed that the main mechanism by which GSK-126 reduces the levels of H3K27me3 in the *RARG* promoter region is its regulation of *RARG* expression (Fig. 2E).

GSK-126 Combined with ATRA has Synergistic Inhibitory Effect on Cell Proliferation

Since GSK-126 restores the ATRA signaling pathway and enhances cellular sensitivity to ATRA, the combination of GSK-126 and ATRA is an important strategy for the treatment of ATRA-resistant HCC. In an exploration of the drug combination's influence on three cellular models, namely Hep3B, HepG2, and SMMC-7721, these lines were exposed to individual treatments of ATRA, GSK-126, as well as a combined therapy at a ratio of 5:1. Utilizing the MTT assay, we discerned the IC_{50} values for both GSK-126

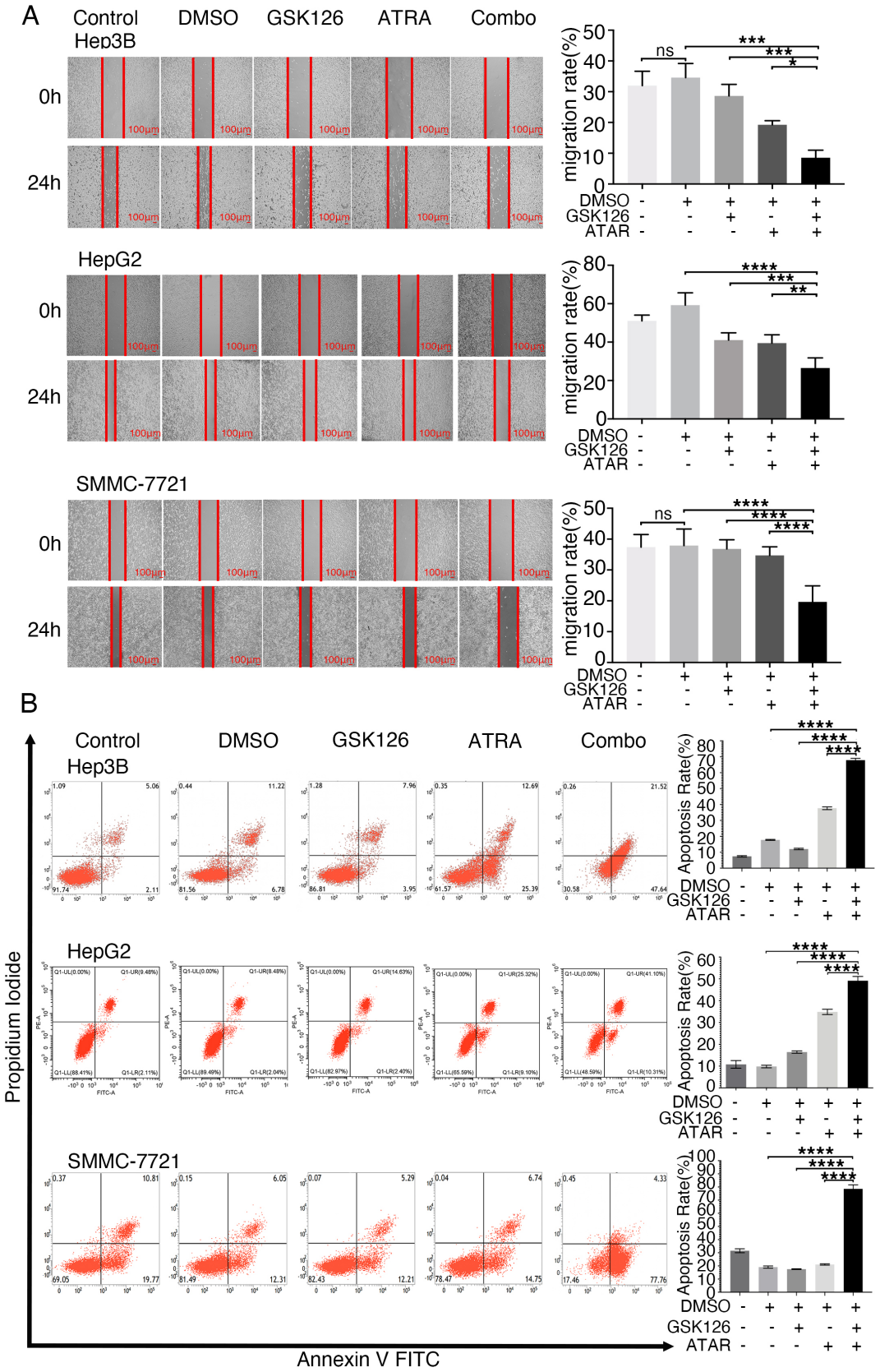

Fig. 4. GSK-126 + all-trans-retinoic acid (ATRA) combination can inhibit migration and induce apoptosis. (A) The combination of GSK-126 and ATRA significantly inhibited migration in Hep3B, HepG2 and SMMC-7721 cell lines. (B) Flow cytometry apoptosis experiment showed that the combination of GSK-126 and ATRA had a synergistic effect on promoting apoptosis of hepatoma cells in Hep3B, HepG2 and SMMC-7721 cell lines. N = 3. ns: not statistically; *$p < 0.05$; **$p < 0.01$; ***$p < 0.001$; ****$p < 0.0001$.

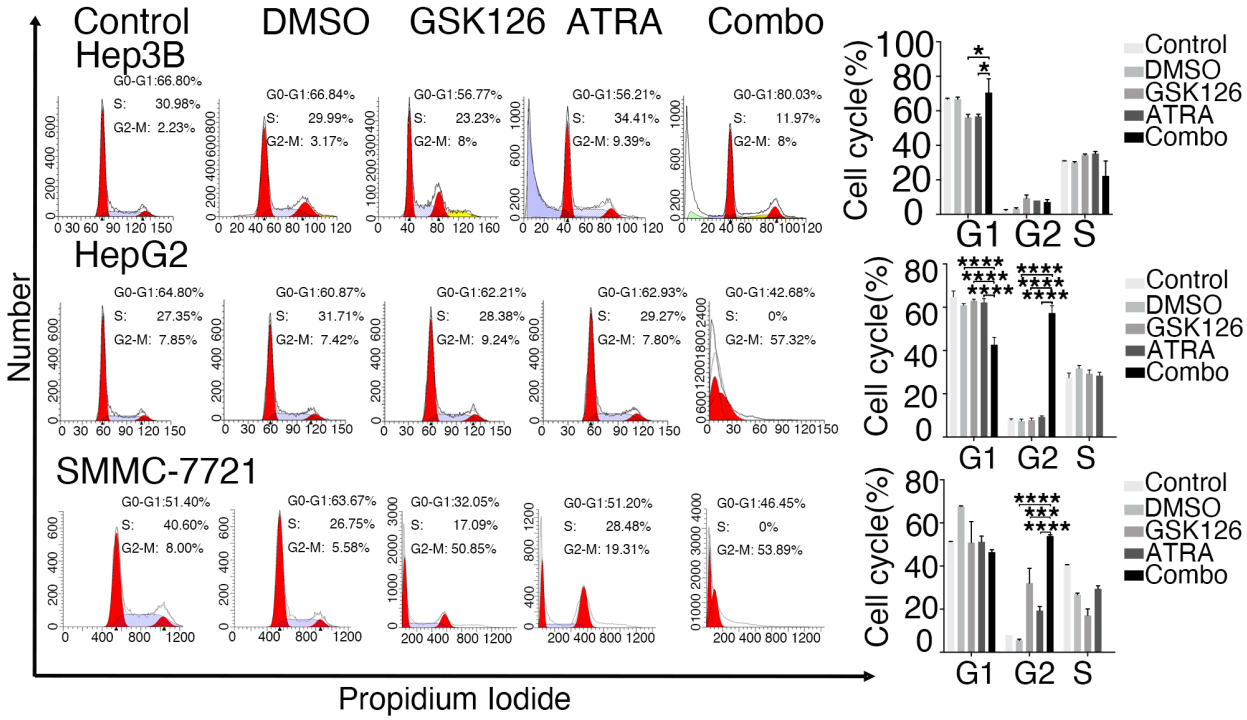

Fig. 5. GSK-126 + ATRA combination can inhibit cell cycle. Flow cytometry showed that the combination of GSK-126 and ATRA altered the cell cycle in Hep3B, HepG2 and SMMC-7721 cell lines. N = 3. Statistical significance is displayed as *$p < 0.05$; ***$p < 0.001$; ****$p < 0.0001$.

and ATRA (Fig. 3A). GSK-126 presented IC_{50} values of 16.88 ± 2.16, 15.313 ± 1.01, and 15.47 ± 0.53 for Hep3B, HepG2, and SMMC-7721 cell lines, respectively. Concurrently, ATRA's IC_{50} measurements on the same lines were 48.37 ± 13.74, 39.5233 ± 2.25, and 65.88 ± 10.49.

Employing the Chou-Talalay methodology [22] for drug combination analysis, our study formulated drug mixtures in constant ratios. Notably, at 50% cell proliferation (fraction affected (Fa) = 0.5), the CI determinations for Hep3B, HepG2, and SMMC-7721 were 0.44 ± 0.039, 0.57 ± 0.027, and 0.65 ± 0.025, as portrayed in Fig. 3B. Such findings underscored a discernible synergy (where CI <1) between GSK-126 and ATRA, even at the minimum concentration levels. The Hep3B line particularly exhibited the most obvious synergistic influence from the drug duo.

From the above synergistic coefficient, it can be seen that the combination of the two drugs has the best synergistic effect in Hep3B cell lines. Moreover, the expression level of RARG is related to the efficacy of ATRA. Therefore, we detected the differences in RARG expression in these three cell lines by western blotting. The results showed that among the three cell lines, Hep3B had the lowest protein expression levels of RARG (Fig. 3C), implying that compared to HepG2 and SMMC-7721 cell lines, the combination of ATRA and GSK-126 exerts a stronger synergistic effect in the Hep3B cell line (Fig. 3B,C) by improving the expression of RARG.

GSK-126 + ATRA Combination can Inhibit Migration, Induce Apoptosis, and Change the Cell Cycle Arrest

First, we used the cell scratch assay to examine the effect of the combination on cell migration ability (Fig. 4A). Compared with the DMSO group ($p < 0.0001$), GSK-126 group ($p < 0.0001$) and ATRA group ($p < 0.0001$), the migration ability of Hep3B, HepG2, and SMMC-7721 cells in the combined treatment group was notably reduced. In essence, the combination of ATRA and GSK-126 demonstrated a potent capacity to impede the migratory tendencies of hepatoma cells.

Then, we detected the apoptosis and cell cycle of SMMC-7721, Hep3B, and HepG2 cells. As shown in Fig. 4B, in the three cell lines, the apoptosis rate was higher in the combination group than in the ATRA alone group ($p < 0.0001$) and GSK126 alone group ($p < 0.0001$). These results indicated that the combination of ATRA and GSK-126 better induce apoptosis than their application alone for the three cell lines.

Cell cycle analysis revealed distinct findings for Hep3B, SMMC-7721, and HepG2 cells. The combination group compared with the monotherapy group, Hep3B cells ($p < 0.05$) were blocked at G1 phase, and HepG2 cells ($p < 0.0001$) and SMMC-7721 cells ($p < 0.0001$) were blocked at G2 phase (refer to Fig. 5).

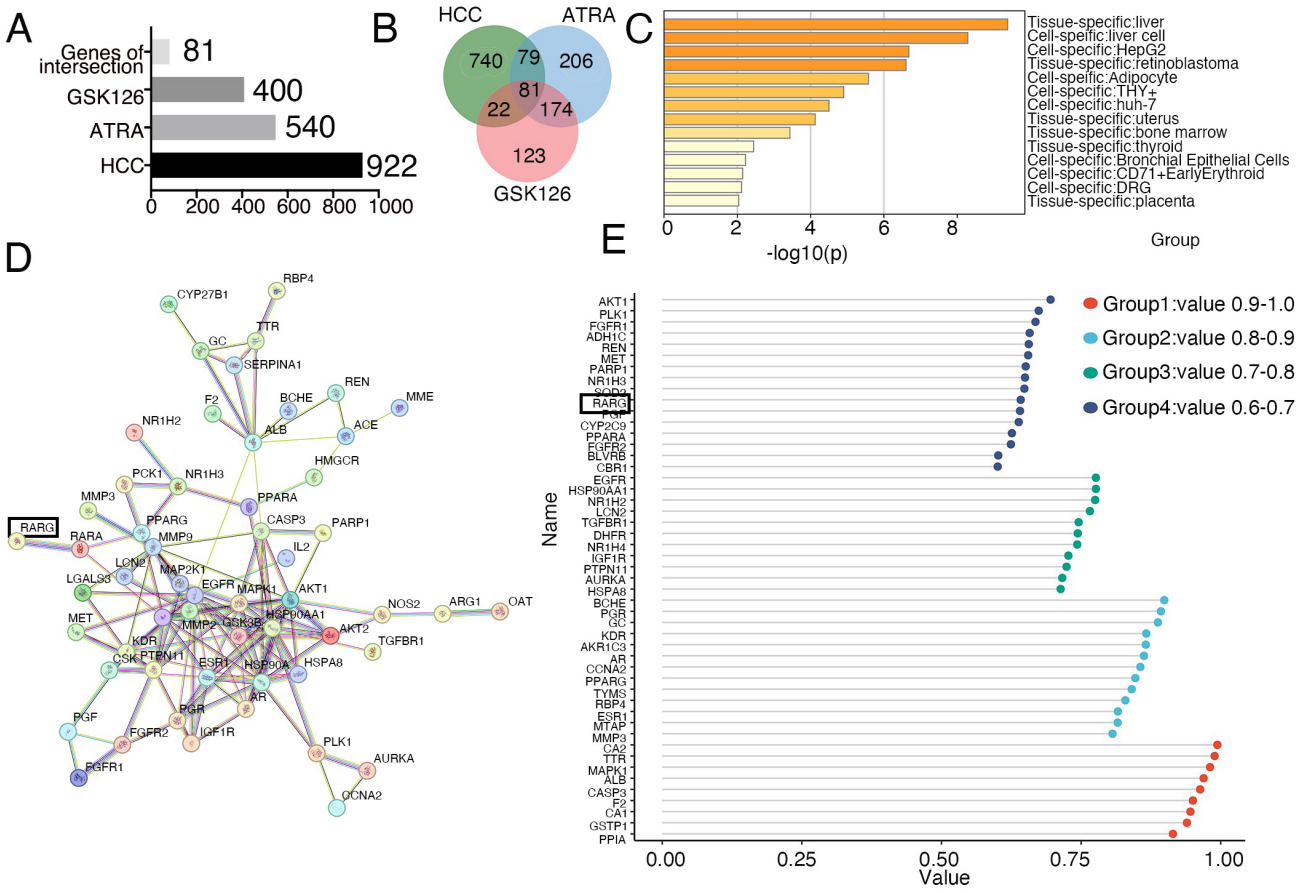

Fig. 6. RARG is a target for GSK-126 combined with all-trans-retinoic acid (ATRA) confirmed by network pharmacology analysis. (A) Number of all targets for HCC, GSK-126 and ATRA. (B) The intersection of HCC, GSK-126, and ATRA targets. (C) The site of action and the disease to be treated, and the cells to be inhibited by the combination. (D) Protein-Protein Interaction Networks (PPI) analysis of 81 targets. (E) Dot chart plot of drug correlation coefficients.

Network Pharmacology Analysis Reveals RARG as a Target for GSK-126 Combined with ATRA

In order to explore the targets of the combination of GSK-126 and ATRA, we used network pharmacology to obtain 922 liver cancer targets, 400 GSK-126 targets, and 540 ATRA targets from the above-mentioned liver cancer database. The intersection of liver cancer-GSK-126-ATRA resulted in 81 targets (Fig. 6A,B). Drawing from the Metascape database, it was discerned that the combined drugs chiefly acted within HCC, with marked specificity for the hepatoma HepG2 cell line, as shown in Fig. 6C. Using the STRING database for PPI analysis of the co-intersecting target genes, we obtained 81 nodes and 285 edges, and the *RARG* gene was associated with the *RARA* gene (Fig. 6D). The correlation coefficient between the target and the drug was obtained through the Pharmmapper database and plotted (Fig. 6E). The correlation coefficient between *RARG* and the two drugs was 0.642.

Discussion

Recent researches have highlighted the potential of ATRA as a drug for combination therapy in solid tumors due to its effects on cell proliferation, differentiation, and apoptosis, coupled with its low toxicity [23,24]. Synergistic effects have been observed in combination therapy involving ATRA with various agents in the fight against cancer [25]. For instance, Sun *et al.* [26] demonstrated that the combination of FOLFOX4 and ATRA improved palliative care efficacy in HCC patients. Lin *et al.* [27] showed a synergistic effect of all-trans-retinoic acid and arsenic trioxide on growth inhibition and apoptosis in human hepatoma, breast cancer, and lung cancer cells *in vitro*.

However, the effectiveness of ATRA can be disrupted during carcinogenesis, necessitating the restoration of the retinoic acid pathway for combination therapy [28,29]. H3K27me3 is closely related to gene silencing, and mutations in the H3K27 methylase EZH2 are widespread in breast cancer, colon cancer, and melanoma [30]. GSK126, a selective histone methylase inhibitor, holds promise for various applications [31]. Zhang *et al.* [32] demonstrated

that GSK-126 can enhance the sensitivity of liver cancer cells to other drugs, such as DNMT, epirubicin (EPB), and mitomycin C (MMC). Previous studies have indicated that combining ATRA with HDAC inhibitors or demethylating agents can enhance cell sensitivity to ATRA [33].

In this study, the combination of GSK-126 and ATRA represents a novel therapeutic approach. GSK-126 not only improves the sensitivity of liver cancer to ATRA but also enhances the killing effect of ATRA on liver cancer cells. This combination offers the advantage of reducing the dosage of ATRA, thereby minimizing the potential for retinoic acid syndrome (RAS) side effects. Moreover, the high selectivity of GSK126 helps mitigate its impact on normal cells. Further exploration is warranted to elucidate the specific mechanism underlying the synergistic effects of ATRA combined with GSK126.

RARs consist of three subtypes: *RARA*, *RARB*, and *RARG* [7]. Studies suggest functional redundancy among RAR subtypes, with single knockout mice exhibiting weaker phenotypes compared to double knockout mice [34,35]. *RARG*, in particular, is selectively expressed in stem cells and plays a role in promoting stem cell renewal [36]. On the other hand, ATRA-activated *RARA* is involved in driving the terminal differentiation of granulocyte and monocyte progenitor cells [37]. The precise roles of RARs and RXRs in mediating ATRA's effects, as well as their potential cooperative or competitive relationship, remain partially understood.

This article provides preliminary clarification that RARG is associated with the insensitivity of HCC to ATRA. RARG may serve as the key receptor for ATRA's therapeutic effects in HCC. Notably, RARG is identified as a specific target in the combination therapy of ATRA and GSK126. Hu *et al*. [38] demonstrated that RARG is one of the overall-survival-related prediction genes, and the protein expression of RARG is reduced in HCC compared with normal tissues. Through GSK-126, which increases the expression of RARG, the combination of ATRA and RARG is shown to enhance tumor suppressor activity.

H3K27me3 plays a crucial role in the development and progression of HCC, and its presence predicts a worse prognosis in patients [39]. The study by Xiao *et al*. [40] explored the effect of EZH2 on PD-L1 from the perspective of H3K27me3. Their mechanistic studies revealed that EZH2 can suppress PD-L1 expression by upregulating the levels of H3K27me3. Many genes are epigenetically silenced by EZH2-mediated H3K27me3, such as WNT10B and ZIC4 [41,42].

The ChIP-seq analysis in this study demonstrated the enrichment of H3K27me3 in the upstream region of the RARG promoter. Abnormal chromatin modification-induced low expression of RARG may be the primary reason for the lack of response to ATRA. Epigenetic reprogramming, exemplified by the use of GSK-126, can reactivate RARG expression and restore the therapeutic effect of ATRA against tumors. This represents one of the mechanisms through which GSK-126 and ATRA exert synergistic effects, highlighting the significance of epigenetic regulation in the context of HCC treatment.

Among the three hepatoma cell lines tested, a notable observation is that the lower the level of RARG expression, the more pronounced the synergistic effect of ATRA and GSK-126 combination therapy. This finding lends further support to the notion that RARG serves as a pivotal target for combination therapy involving ATRA and GSK-126. The expression of RARG holds promise as a potential predictive biomarker for identifying HCC patients who stand to benefit from this synergistic approach. Additionally, our upcoming investigations will delve into the toxic and side effects, specific pharmacological outcomes, and drug metabolism associated with the combined administration of these drugs. This research aims to furnish theoretical support for the clinical application of the combination therapy of ATRA and GSK-126.

Conclusion

The study has effectively showcased that the synergistic combination of GSK-126 and ATRA inhibits the growth of HCC cells and heightens the sensitivity of these cells through the upregulation of RARG expression. This discovery provides a promising foundation for personalized HCC treatment strategies.

Availability of Data and Materials

The datasets used and/or analyzed during the current study are available from the corresponding author on reasonable request.

Author Contributions

ZDL was responsible for the design of the study, conduction of the experiment, analysis of the data and completion of the manuscript. YXZ conceived the project, planned and guided the research, and supervised the study. YXZ participated in the drafting of the manuscript, grasped the quality of the article, and revised the content of the article. Both authors contributed to the editing of the manuscript. Both authors read and approved the final manuscript. Both authors were fully involved in the work and agreed to take responsibility for all aspects of the work.

Ethics Approval and Consent to Participate

Not applicable.

Acknowledgment

Not applicable.

Funding

This work was supported by Zhejiang Public Welfare Applied Technology Research Project (LGD22H160004), China Postdoctoral Science Foundation (2018M633092) and the key Laboratory of Medical Electronics and Digital Health of Zhejiang Province.

Conflict of Interest

The authors declare no conflict of interest.

Supplementary Material

Supplementary material associated with this article can be found, in the online version, at https://doi.org/10.24976/Discov.Med.202436184.97.

References

[1] Yang C, Zhang H, Zhang L, Zhu AX, Bernards R, Qin W, *et al*. Evolving therapeutic landscape of advanced hepatocellular carcinoma. Nature Reviews. Gastroenterology & Hepatology. 2023; 20: 203–222.

[2] Ding X, He M, Chan AWH, Song QX, Sze SC, Chen H, *et al*. Genomic and Epigenomic Features of Primary and Recurrent Hepatocellular Carcinomas. Gastroenterology. 2019; 157: 1630–1645.e6.

[3] Gao Q, Wang ZC, Duan M, Lin YH, Zhou XY, Worthley DL, *et al*. Cell Culture System for Analysis of Genetic Heterogeneity Within Hepatocellular Carcinomas and Response to Pharmacologic Agents. Gastroenterology. 2017; 152: 232–242.e4.

[4] Khedr M, Barakat N, Mohey El-Deen I, Zahran F. Impact of preconditioning stem cells with all-trans retinoic acid signaling pathway on cisplatin-induced nephrotoxicity by down-regulation of TGFβ1, IL-6, and caspase-3 and up-regulation of HIF1α and VEGF. Saudi Journal of Biological Sciences. 2022; 29: 831–839.

[5] Shi J, Sun J, Liu C, Chai Z, Wang N, Zhang H, *et al*. All-trans-retinoic acid (ATRA) plus oxaliplatin plus 5-fluorouracil/leucovorin (FOLFOX) versus FOLFOX alone as palliative chemotherapy in patients with advanced hepatocellular carcinoma and extrahepatic metastasis: study protocol for a randomized controlled trial. Trials. 2019; 20: 245.

[6] Ni X, Hu G, Cai X. The success and the challenge of all-trans retinoic acid in the treatment of cancer. Critical Reviews in Food Science and Nutrition. 2019; 59: S71–S80.

[7] Chambon P. A decade of molecular biology of retinoic acid receptors. FASEB Journal. 1996; 10: 940–954.

[8] Brown G. Retinoic acid receptor regulation of decision-making for cell differentiation. Frontiers in Cell and Developmental Biology. 2023; 11: 1182204.

[9] Brown G. Deregulation of All-*Trans* Retinoic Acid Signaling and Development in Cancer. International Journal of Molecular Sciences. 2023; 24: 12089.

[10] Chen X, Wang F, Zhang Y, Teng W, Cao P, Ma X, *et al*. A novel NPM1-RARG-NPM1 chimeric fusion in acute myeloid leukaemia resembling acute promyelocytic leukaemia but resistant to all-trans retinoic acid and arsenic trioxide. British Journal of Cancer. 2019; 120: 1023–1025.

[11] Zhang J, Lee D, Dhiman V, Jiang P, Xu J, McGillivray P, *et al*. An integrative ENCODE resource for cancer genomics. Nature Communications. 2020; 11: 3696.

[12] Entezari M, Taheriazam A, Paskeh MDA, Sabouni E, Zandieh MA, Aboutalebi M, *et al*. The pharmacological and biological importance of EZH2 signaling in lung cancer. Biomedicine & Pharmacotherapy. 2023; 160: 114313.

[13] Liu Y, Yang Q. The roles of EZH2 in cancer and its inhibitors. Medical Oncology. 2023; 40: 167.

[14] Kim KH, Roberts CWM. Targeting EZH2 in cancer. Nature Medicine. 2016; 22: 128–134.

[15] Kagiyama Y, Fujita S, Shima Y, Yamagata K, Katsumoto T, Nakagawa M, *et al*. CDKN1C-mediated growth inhibition by an EZH1/2 dual inhibitor overcomes resistance of mantle cell lymphoma to ibrutinib. Cancer Science. 2021; 112: 2314–2324.

[16] Li C, Song J, Guo Z, Gong Y, Zhang T, Huang J, *et al*. EZH2 Inhibitors Suppress Colorectal Cancer by Regulating Macrophage Polarization in the Tumor Microenvironment. Frontiers in Immunology. 2022; 13: 857808.

[17] Wang C, Chen X, Liu X, Lu D, Li S, Qu L, *et al*. Discovery of precision targeting EZH2 degraders for triple-negative breast cancer. European Journal of Medicinal Chemistry. 2022; 238: 114462.

[18] Yap TA, Winter JN, Giulino-Roth L, Longley J, Lopez J, Michot JM, *et al*. Phase I Study of the Novel Enhancer of Zeste Homolog 2 (EZH2) Inhibitor GSK2816126 in Patients with Advanced Hematologic and Solid Tumors. Clinical Cancer Research. 2019; 25: 7331–7339.

[19] Li C, Wang Y, Gong Y, Zhang T, Huang J, Tan Z, *et al*. Finding an easy way to harmonize: a review of advances in clinical research and combination strategies of EZH2 inhibitors. Clinical Epigenetics. 2021; 13: 62.

[20] Bardou P, Mariette J, Escudié F, Djemiel C, Klopp C. jvenn: an interactive Venn diagram viewer. BMC Bioinformatics. 2014; 15: 293.

[21] von Mering C, Huynen M, Jaeggi D, Schmidt S, Bork P, Snel B. STRING: a database of predicted functional associations between proteins. Nucleic Acids Research. 2003; 31: 258–261.

[22] Chou TC. Drug combination studies and their synergy quantification using the Chou-Talalay method. Cancer Research. 2010; 70: 440–446.

[23] Colita A, Tanase AD, Tomuleasa C, Colita A. Hematopoietic Stem Cell Transplantation in Acute Promyelocytic Leukemia in the Era of All-Trans Retinoic Acid (ATRA) and Arsenic Trioxide (ATO). Cancers. 2023; 15: 4111.

[24] Liang C, Qiao G, Liu Y, Tian L, Hui N, Li J, *et al*. Overview of all-trans-retinoic acid (ATRA) and its analogues: Structures, activities, and mechanisms in acute promyelocytic leukaemia. European Journal of Medicinal Chemistry. 2021; 220: 113451.

[25] Altucci L, Gronemeyer H. The promise of retinoids to fight against cancer. Nature Reviews. Cancer. 2001; 1: 181–193.

[26] Sun J, Mao F, Liu C, Zhang F, Jiang D, Guo W, *et al*. Combined FOLFOX4 with all-trans retinoic acid versus FOLFOX4 with placebo in treatment of advanced hepatocellular carcinoma with extrahepatic metastasis: a randomized, double-blind comparative study. Signal Transduction and Targeted Therapy. 2023; 8: 368.

[27] Lin LM, Li BX, Xiao JB, Lin DH, Yang BF. Synergistic effect of all-trans-retinoic acid and arsenic trioxide on growth inhibition and apoptosis in human hepatoma, breast cancer, and lung cancer cells in vitro. World Journal of Gastroenterology. 2005; 11: 5633–5637.

[28] Chlapek P, Slavikova V, Mazanek P, Sterba J, Veselska R. Why Differentiation Therapy Sometimes Fails: Molecular Mechanisms of Resistance to Retinoids. International Journal of Molecular Sciences. 2018; 19: 132.

[29] Geoffroy MC, Esnault C, de Thé H. Retinoids in hematology: a timely revival? Blood. 2021; 137: 2429–2437.

[30] Duan R, Du W, Guo W. EZH2: a novel target for cancer treatment. Journal of Hematology & Oncology. 2020; 13: 104.

[31] Zhang Q, Chen X, Hu X, Duan X, Wan G, Li L, *et al*. Covalent inhibitors of EZH2: Design, synthesis and evaluation. Biomedicine & Pharmacotherapy. 2022; 147: 112617.

[32] Zhang L, Li HT, Shereda R, Lu Q, Weisenberger DJ, O'Connell C, *et al*. DNMT and EZH2 inhibitors synergize to activate therapeutic targets in hepatocellular carcinoma. Cancer Letters. 2022; 548: 215899.

[33] Touma SE, Goldberg JS, Moench P, Guo X, Tickoo SK, Gudas LJ, *et al*. Retinoic acid and the histone deacetylase inhibitor trichostatin a inhibit the proliferation of human renal cell carcinoma in a xenograft tumor model. Clinical Cancer Research. 2005; 11: 3558–3566.

[34] Kastner P, Grondona JM, Mark M, Gansmuller A, LeMeur M, Decimo D, *et al*. Genetic analysis of RXR alpha developmental function: convergence of RXR and RAR signaling pathways in heart and eye morphogenesis. Cell. 1994; 78: 987–1003.

[35] Merki E, Zamora M, Raya A, Kawakami Y, Wang J, Zhang X, *et al*. Epicardial retinoid X receptor alpha is required for myocardial growth and coronary artery formation. Proceedings of the National Academy of Sciences of the United States of America. 2005; 102: 18455–18460.

[36] Brown G. Antagonizing RARγ Drives Necroptosis of Cancer Stem Cells. International Journal of Molecular Sciences. 2022; 23: 4814.

[37] Xu S, Wang S, Xing S, Yu D, Rong B, Gao H, *et al*. KDM5A suppresses PML-RARα target gene expression and APL differentiation through repressing H3K4me2. Blood Advances. 2021; 5: 3241–3253.

[38] Hu B, Yang XB, Sang XT. Molecular subtypes based on immune-related genes predict the prognosis for hepatocellular carcinoma patients. International Immunopharmacology. 2021; 90: 107164.

[39] Kusakabe Y, Chiba T, Oshima M, Koide S, Rizq O, Aoyama K, *et al*. EZH1/2 inhibition augments the anti-tumor effects of sorafenib in hepatocellular carcinoma. Scientific Reports. 2021; 11: 21396.

[40] Xiao G, Jin LL, Liu CQ, Wang YC, Meng YM, Zhou ZG, *et al*. EZH2 negatively regulates PD-L1 expression in hepatocellular carcinoma. Journal for Immunotherapy of Cancer. 2019; 7: 300.

[41] Zhang S, Jiang M, Cao H, Xiong J, Xu J. CTB-193M12.5 Promotes Hepatocellular Carcinoma Progression via Enhancing NSD1-Mediated WNT10B/Wnt/β-Catenin Signaling Activation. Journal of Hepatocellular Carcinoma. 2022; 9: 553–569.

[42] Chen W, Tang D, Tang D, Dai Y. Epigenetic silencing of ZIC4 contributes to cancer progression in hepatocellular carcinoma. Cell Death & Disease. 2020; 11: 906.